Polish Society of Composite Materials
Polskie Towarzystwo Materiałów Kompozytowych

https://doi.org/10.62753/ctp.2021.07.4.4

21: 4 (2021) 161-168

COMPOSITES THEORY AND PRACTICE
ISSN: 2084-6096
ISSN (online): 2299-128X

Marek Grabowy[1]*, Yurii Delikhovskyi[2], Agnieszka Wilk[2]*, Zbigniew Pędzich[2]

[1] IEN Institute of Power Engineering, ul. Mory 8, 01-330 Warsaw, Poland, Ceramic Branch CEREL, ul. Techniczna 1, 36-040 Boguchwała, Poland
[2] AGH – University of Science and Technology, Faculty of Materials Science and Ceramics, Department of Ceramics and Refractories al. A. Mickiewicza 30, 30-059 Krakow, Poland
** Corresponding authors. E-mail: wilka@agh.edu.pl; grabowy@cerel.pl*

Received (Otrzymano) 24.11.2021

IMPROVEMENT OF FRACTURE TOUGHNESS IN DENSE ATZ COMPOSITES PREPARED FROM ZIRCONIA POWDERS WITH DIFFERENT YTTRIA CONTENT

Alumina toughened zirconia (ATZ) composites with 2.3 vol.% Al_2O_3(ATZ-B) and 12.3 vol.% Al_2O_3(ATZ-10) were fabricated. The used starting zirconia powders were prepared as a mixture of powders with different yttria content. The alumina additive was commercially available Al_2O_3 powder. The specific preparation method and optimized sintering conditions allowed us to achieve ATZ products with exceptional properties. These properties were compared with 3Y-TZP sintered samples prepared from commercial powder (Tosoh). The structural and mechanical properties of the investigated ATZ composites were systematically studied. The microstructures were observed by scanning electron microscopy (SEM) on polished and thermally etched surfaces, then the micrographs were binarized and subjected to stereological analysis. Dense (> 99% of relative density), uniform and pore-free microstructures with homogeneously distributed Al_2O_3 inclusions without any visible agglomerates were obtained. The Vickers hardness and Young's modulus were enhanced according to the rule of mixtures for the composites. The mechanical behaviour was especially oriented towards increasing the fracture toughness. The K_{1C} parameter reached the extraordinary value of 12.7 MPa·m$^{1/2}$ for ATZ-B and 9.8 MPa·m$^{1/2}$ for ATZ-10. Comparatively, K_{1C} of the 3Y-TZP reference material was 5.1 MPa·m$^{1/2}$. The mechanisms contributing to the increase in K_{1C} were identified to explain the reason for such a large improvement in the fracture toughness. The investigations were particularly focused on crack propagation analysis. The identified mechanisms include crack path deviation and mixed transgranular-intragranular crack migration (crack bridging), crack propagation through theAl_2O_3 grains and frequent changes in the fracture propagation directions of a high angle (close to even 90°). Nevertheless, the occurrence of t→m (tetragonal to monoclinic) transformation of the ZrO_2 phase was considered to be the main toughening factor. Due to the specific method of preparation, leading to an intensification of yttrium diffusion during sintering, the final microstructure revealed very small grains of a tetragonal zirconia phase. These grains exhibited high transformability, which was the main reason for the distinctin crease in fracture toughness.

Keywords: ATZ composites, fracture toughness, toughening mechanisms, crack propagation

INTRODUCTION

Brittleness is one of the main problems of all ceramic materials, which limits the areas of their application. Focusing on this aspect, in the 1970s Garvie et al. [1] discovered an important advantage of zirconium oxide ZrO_2 ceramics – the transformation toughening effect. This ability to transform from a high temperature tetragonal crystal structure to a monoclinic one, dissipates energy and limits crack propagation and finally gives the material a new level of strength and toughness.

The tetragonal t-form of the ZrO_2 phase can be obtained by heating zirconia crystals to 1700°C, but during cooling recovery to a monoclinic m-phase appears [2]. In order to increase the metastability of the zirconium t-phaseatroom temperature, different oxide additives such as Gd_2O_3, MgO, CeO_2 and the most popular – Y_2O_3- are used [3-6]. Yttrium-tetragonal zirconia ceramics, called Y-TZP, due to their excellent mechanical properties, biocompatibility and chemical resistance, have found their use in biomedical applications as dental and orthopaedic implants [6, 7]. It is well known that the use of composite materials allows one to combine and improve the properties of individual components. In order to enhance the mechanical properties of zirconia materials, numerous research works have been carried out on developing ATZ-composites, in which the ZrO_2 matrix is toughened by Al_2O_3 additives (ATZ-alumina toughened zirconia) [8, 9].

Alumina-based ceramics are known for their good biocompatibility and resistance to corrosion, good wear resistance and excellent compression strength of 4000 MPa (Vickers hardness reaching 2000 HV). Nevertheless, they simultaneously have low bending strength at the level of 600 MPa and fracture toughness of 5 MPa·m$^{1/2}$, which limits their areas of application [10, 11]. A comparison of the properties of these materials is presented in Table 1 [12]. Most of the properties of materials can be changed in wide range depending on

the content of the individual components, particle size and shape [13, 14], processing and preparation of the mixtures, sintering temperature and time [9, 15-17]. Knowledge about the influence of each of them is essential for the correct design of the desired product properties.

TABLE 1. **Important properties of selected materials (according to [12, 18])**

Materials	Density [g/cm^3]	Hardness [HV]	Compressive strength [MPa]	Bending strength [MPa]	Fracture toughness [MPa·m^{12}]
Al_2O_3	>3.97	1800-2000	4000	600	4-5
ZrO_2 (Y-TZP)	6.53	1400	3000-4000	800-1100	10
ATZ 80%ZrO_2-20%Al_2O_3	5.4	1400	2500	800-1200	5

The ability of materials to resist crack propagation is one of the most important mechanical parameters, and in order to describe it, the critical stress intensity factor (K_{1C}) is used. The higher the K_{1C} parameter value is, the better the resistance to crack propagation [19]. There are a few methods that are commonly used to improve zirconia ceramic toughening strength. The predominant toughening effect is the t→m (tetragonal to monoclinic) transformation mechanism [20-22]. When the crack tip interacts with tetragonal zirconia particles, a stress--induced t→m transformation occurs. The metastable tetragonal phase undergoes a martensite phase transformation and the accompanying lattice expansion absorbs the crack energy, thereby improving toughness [23-25]. According to [21-23] those phenomena constitute the predominant toughening mechanism in zirconia-based ceramics.

Along with the above, the manufacturing process of composite materials also can significantly improve fracture toughness. Celli et al. [26] prepared the composite by adding corundum to the zirconium oxide matrix (20 wt.% Al_2O_3 + 80 wt.% ZrO_2 (3Y-TZ)) and obtained a stress intensity factor value of 5.0±0.2 MPa·m$^{1/2}$, which is higher than that of the used starting Al_2O_3 and ZrO_2 (3Y-TZ) materials (4.2±0.4 and 4.3±0.1 MPa·m$^{1/2}$, respectively). Magnani et al. [27] also showed that the preparation of the composite and changing its proportions has an influence on toughness. In addition to different amounts of corundum additives, it has been shown that the content of t-phase stabiliser and other additives have an impact on the fracture toughness. In published studies, for a 49.5 wt.% Al_2O_3 + 50 wt.% ZrO_2 (with 2 mol% yttria) composite, with an 0.5 wt.% Cr_2O_3 additive, a significant increase in the K_{1C} parameter up to 9.1±0.8 MPa·m$^{1/2}$ was achieved. It was also found that the toughness of the material can be highly affected by the employed sintering parameters. For example, a decrease in toughness was observed for additional 1450°C × 2 h post-hot isostatic treatment. This heating leads to slight grain growth and thus to a spontaneous t→m transformation to some extent, which reduced the amount of t→phase available for transformation; therefore, as light K_{1C} decrease from 6.0 ±0.1 to 5.8±0.1 MPa·m$^{1/2}$ was observed. Danilenko et. al [15] investigated the effect of the nano powder synthesis method on the mechanical properties of ATZ composites. It was reported that a higher fracture toughness can be achieved when the starting powders are obtained using the co-precipitation method rather than the traditional ball milling mixing method. For 1.0 wt.% Al_2O_3 + 99.0 wt.% ZrO_2 (3Y-TZ) composites, the obtained fracture toughness reaches 11.2 ±0.6 and 6.1±0.3 MPa·m$^{1/2}$, respectively for the two employed methods. As was reported, the main mechanisms that caused this difference were the formation of complex multilevel composite structures such as Al^{3+} ion segregation on the zirconia grain boundaries and grain boundary enrichment with alumina inclusions for the material obtained by the co-precipitation method. Those phenomena caused new crack inhibition mechanisms to appear – more intensive crack bridging, crack deflection and transgranular propagations. Tekeli et al. [28] investigated the effect of various amounts of the Al_2O_3 addition on the fracture toughness of cubic zirconium 8YSCZ/Al_2O_3 composites; hence, the t→m transformation influence was partly eliminated by c→m (cubic to monoclinic) transformation. It was concluded that the K_{1C} values increased from 1.5 MPa·m$^{1/2}$ to 2.41 MPa·m$^{1/2}$ as the Al_2O_3 content increased from 0 to 10 wt.%. The relation between fracture toughening and the Al_2O_3 content in terms of grain size reduction, crack deflection at the crack tip and the residual stress in the composites was explained.

Another relation between the high level of crack deviations and toughening effect was explained by Nevarez-Rascon et al. [14]. Crack tip meandering increases the fracture specific area; as a result, energy absorption is increased, which in turn raises the fracture toughness. According to Chai et al. [29], the formation of deflections is related to the blockage of hard particles during crack expansion in the composite matrix. In addition, all those mechanisms mentioned above increase the number of trans granular fractures, which also results in improvement in the fracture toughness [30, 31].

The emerging discrepancies regarding the influence of the Al_2O_3 addition to theZrO_2 matrix and the differences in the obtained parameters values result from the diversity of the starting materials and production methods. Those factors undoubtedly affect the final microstructure and phase structure of the ATZ composites and thus to a large extent determine the final properties.

In the presented work, the properties of ATZ composites obtained according to a specific preparation route from ZrO_2 powders with different Y_2O_3 contents are investigated and discussed. The sintering conditions were chosen to achieve an increase in fracture toughness. The microstructure, phase composition and the basic mechanical properties were also studied.

 All rights reserved

Additionally, an attempt was made to identify the factors which bring about the phenomena of increasing the fracture toughening effect by means of crack propagation analysis.

EXPERIMENT

Materials

Two zirconium oxide powders obtained by the coprecipitation/calcination method were used as the starting materials – pure nanometric ZrO_2 and yttria-zirconia solid solution powders containing a 4 mol.% Y_2O_3 stabilizer. A detailed description of the utilized methods and the individual preparations tages of the powders are presented elsewhere [32].

The base material (hereinafter referred to as ATZ-B) was prepared from the obtained 3 mol.% yttria--tetragonal ZrO_2 powders with the addition of commercial 2.3 vol.% alumina (nanometric Al_2O_3 powder TM-DAR, Taimicron, Taimei Chemicals). Based on the aforementioned ATZ-B powder, by increasing the Al_2O_3 volume content to 12.3%, the composite denoted as ATZ-10 was obtained. Additionally, for comparative purposes, reference samples were prepared from commercially available zirconia powder with a content of 3 mol.% Y_2O_3, hereinafter called T (3Y-TZP).

The 3 mol.% Y_2O_3-ZrO_2 with the Al_2O_3 powder mixture was homogenized in an attritor mill for 60 minutes in isopropyl alcohol as the mixing agent. Subsequently, the powders were dried, uniaxially prepressed under a pressure of 50 MPa in a Specac hydraulic press and then subjected to CIP (cold isostatic pressing) under a pressure of 200 MPa. The green bodies were conventionally sintered in air atmosphere in the presence of a zirconia powder bed (high-temperature Nabertherm furnace) with a slow heating rate to the maximum temperature of 1450°C and held for 1.5 hours at this temperature.

From each group of the investigated materials (ATZ-B, ATZ-10 and T) several samples were randomly selected and embedded in resin to prepare for microstructure analysis. In the next step, the samples were subjected to grinding and machine polishing by diamond discs with the following gradations #120, #600 and #200 (Diamond Pad, Struers). The final surface treatment was performed with an MD-Chem polishing cloth (Struers) using 1 μm diamond polishing paste. Finally, the specimens were subjected to thermal etching at the temperature of 1200°C for 45 minutes.

Methods

The densities of the specimens were determined according to the Archimedes method. Their theoretical densities were calculated based on the rule of mixtures. The phase compositions of the ATZ-B, ATZ-10 and T materials were analysed by an X-ray diffractometer (X'Pert Pro, EMPYREAN system, PANalytical). The peaks corresponding to tetragonal zirconia, monoclinic zirconia and alumina were identified using JCPDS files. Rietveld refinement allowed quantification of the amount of constituent phases. The microstructure of the investigated materials and the crack propagation were observed on polished and thermally-etched samples using a Nova NanoSEM 200 high-resolution scanning electron microscope equipped with a field-emission gun produced by FEI. Moreover, the obtained micrographs were manually binarized and then analyse demploying the ImageJ program.

The flexural strength of the materials was determined on a Zwick/Roell Z020 universal testing machine using the three-point biaxial test [33-35]. The measurements of hardness and critical stress intensity factor K_{1C} of the ATZ composites and the reference material were performed by means of the Vickers indentation method (Futur-Tech hardness tester FV-700) at room temperature applying a load of 9.81 N. The propagation of Palmquist cracks was analysed under the load of 49.05 N. The K_{1C} parameter was determined based on the Niihara equation and measurement of the Palmquist cracks and indentation sizes [36]. The measurements were made immediately after making the indents to avoid possible changes in the length of the cracks under the influence of environmental conditions (humidity, temperature) and a minimum of 10 indents were made on each randomly selected sample.

RESULTS AND DISCUSSION

Table 2 shows the quantitative phase compositions of the materials after sintering, estimated by XRD analysis using Rietveld refinement. From the XRD results it is evident that all the samples exhibit a highly crystalline structure. It was identified that ATZ-10 was mainly composed of the tetragonal zirconia t-phase with a minor content of monoclinic zirconia m-phase and alumina phase.

TABLE 2. **Phase content of studied materials in initial state (after sintering) estimated by Rietveld refinement**

After sintering					
Content [wt. %] / Composite	m-ZrO_2	$\frac{m}{m+t}\cdot 100\%$	t-ZrO_2	$\frac{t}{m+t}\cdot 100\%$	Al_2O_3
ATZ-B	42.6	43.2	55.9	56.8	1.5
ATZ-10	10.9	11.9	80.8	88.1	8.3
3Y-TZP	-		100	100	-

m/(m+t) and t/(m+t) are m-phase content and t-phase content in relation to total amount of ZrO_2 phase, respectively.

The Al_2O_3 mass content for ATZ-10 is 8.3 wt.% and represents a volume content of 11.5 vol.%, which corresponds well to the actual desired composition. The analysis confirmed the purity of the composites and the absence of any secondary phases derived from zirconia

and alumina interactions. In the 3Y-TZP reference material, as was expected, only the zirconia t-phase was present. The significant amount of the m-phase present in the ATZ-B composite was unexpected. As mentioned in the authors' previous article [32], this is probably related to the method of powder preparation (from a mixture of powders with differences in yttria content) and the specific rate of heat treatment, which was tailored to obtain the best mechanical parameters of the composites. Moreover, this specific phase composition may indicate the high transformability of the ZrO_2t-phase.

Figure 2 presents the SEM micrographs of the microstructure of the investigated materials. In the bright-grain zirconia matrix the alumina inclusions can be observed, which are seen as dark phases. Both the composites and the reference material are characterized by a dense, pore-free microstructure with a high value of relative density (over 99%). The least present phase (Al_2O_3) is homogenously dispersed in the ZrO_2 matrix without evident agglomerations. Those observations allow us to assume that the methodology used for sample preparation produces samples with a dense, fine and homogeneous microstructure.

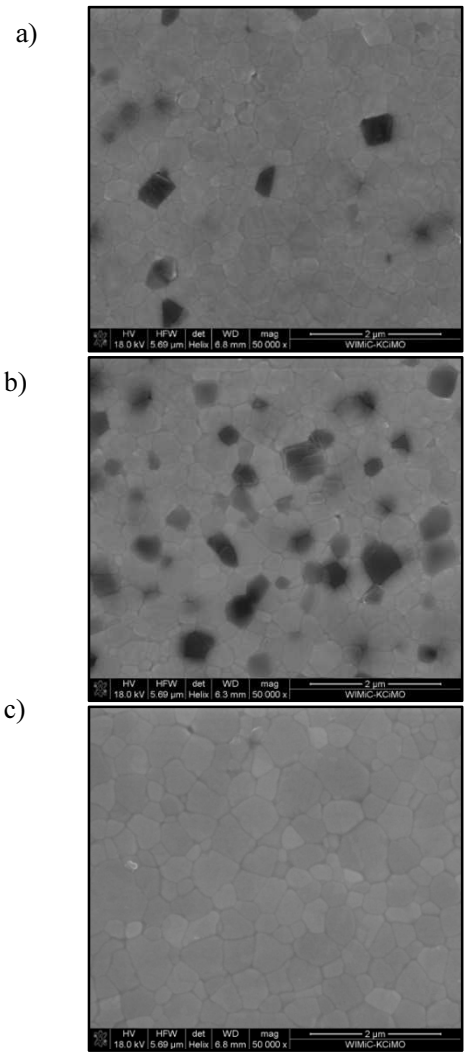

Fig. 2. SEM micrographs of microstructures of: a) ATZ-B, b) ATZ-10, c) T

The grain sizes and phase fraction of the individual components in the investigated materials, obtained from analysis of the binarized SEM micrographs by means of stereological methods are listed in Table 3. Sufficiently accurate average results from the measurements of at least 1000 grains were reported. As presented, the linear grain sizes slightly decrease with an increasing Al_2O_3 content. According to Nevarez-Rascon et al. [14] the grain size reduction in ATZ composites is caused due to the fact that Al_2O_3 acts as an inhibitor of grain growth during sintering processes. Similar results were obtained in the study conducted by Tekeli [28], who indicated that a greater amount of Al_2O_3 addition inhibits densification and grain growth by reducing the mobility and diffusivity (migration) of atoms at the grain boundaries. Therefore, by introducing the Al_2O_3 phase and optimizing the sintering conditions, it is possible to obtain a fine-grained microstructure. Regardless, in both the ATZ-B and ATZ-10 composites the Al_2O_3 grains are slightly larger than the ZrO_2 matrix grains (Table 3). The volume fractions of the Al_2O_3 phase in the ATZ composites obtained as a result of the stereological analysis are almost identical to their real, designed proportions.

TABLE 3. **Microstructure parameters obtained by stereological analysis in ImageJ program**

Material	Component	Phase fraction [%]	Average linear grain size [μm]	Average grain surface [μm^2]
ATZ-B	ZrO_2	98	0.33 ± 0.14	0.08 ±0.06
	Al_2O_3	2	0.48 ± 0.09	0.15 ±0.05
ATZ-10	ZrO_2	89	0.32 ± 0.15	0.08 ±0.06
	Al_2O_3	11	0.38 ± 0.15	0.12 ±0.08
T	ZrO_2	100	0.41 ± 0.15	0.12 ±0.09

The calculated theoretical density, determined apparent and relative density, as well as important mechanical properties are reported in Table 4. Concerning the mechanical properties of the composites, some of the obtained results are related to the rule of mixtures. Considering the Young's modulus for ZrO_2 (210 GPa) [17] and Al_2O_3 (400 GPa) [17], according to the rule of mixtures, this parameter for the investigated composites can reach a maximum value of around 250 GPa. The measured Young's modulus values for ATZ-10 (240±15 GPa) and ATZ-B (220 ±10 GPa) are consistent with the theoretical predictions. Similar observations can be concluded for the Vickers hardness (HV) of the analysed samples, which also changes according to the rule of mixtures (Table 4). Detailed analysis of the changes in those and other mechanical properties is not the main subject of this paper and was discussed in previous work [32].

 All rights reserved

TABLE 4. **Density and basic mechanical properties of investigated ATZ composites and 3Y-TZP reference material**

Material	Theoretical density [g/cm^3]	Apparent density [g/cm^3]	Relative density [%]	Hardness HV [GPa]	K_{1C} [MPa·m$^{1/2}$]	Young's modulus [GPa]	Flexural strength [GPa]
ATZ-B	6.01	5.97	99.3	12.0 ±2.6	12.7±0.8	220±10	780±50
ATZ-10	5.81	5.78	99.5	13.1 ±2.6	9.8±1.4	240±15	1000±100
T	6.10	6.07	99.7	13.8 ±3.0	5.1±0.1	210±10	1040±120

Nevertheless, it is worth noting and emphasizing that the fracture toughness of the investigated ATZ composites was much more improved than it would appear from the rule of mixtures. The K_{1C} parameter reached a value of 12.7±0.8 MPa·m$^{1/2}$ for ATZ-B and 9.8±1.4 MPa·m$^{1/2}$ for ATZ-10, respectively. To the authors' knowledge, the highest K_{1C} reported in the literature for ATZ composites with a similar composition state the values of 11.2±0.6 MPa·m$^{1/2}$ [15], 6.7±0.9 MPa·m$^{1/2}$ [37], ~6.5 MPa·m$^{1/2}$ [16] and 4.8-5.2 MPa·m$^{1/2}$ [38]. Some publications speculate that the absolute toughness determined by the Vickers indentation technique might be overestimated; however, this method has gained general approval for estimating fracture toughness values [39]. In order to explain such a large increase in K_{1C}, an attempt was made to identify and determine the additional mechanisms that are present in the ATZ composites and can contribute to the improvement intheir fracture toughness. The investigations were particularly focused on crack propagation analysis.

Figure 3 shows the crack propagation after Vickers indentation, where the arrows indicate the various mechanisms that improve the fracture toughness and have a positive effect on increasing the value of K_{1C}. The identified, specified mechanisms include crack path deviation and mixed transgranular-intragranular crack migration (crackbridging and deflection processes). The crack deflection process is well-known and frequently encountered in ATZ-type composites [14, 15, 30]. Black arrows (Fig. 3) mark are as with a high level of crack meandering, which is particularly strong in ATZ composites. The homogenously dispersed Al_2O_3 grains enhanced the crack deviations. In contrast, in the 3Y-TZP reference material the crack propagates through the material almost in a straight path. Grey and white arrows indicate crack attraction by the Al_2O_3 grains for transgranular and intergranular propagation, respectively. The encountered mechanisms lead to energy loss and improvement in the fracture toughness of the ATZ composites [30, 31]. Nonetheless, earlier studies [40-42] confirmed an increase in K_{1C} by a maximum value of 0.5 MPa·m$^{1/2}$ resulting from crack deflection, and up to 0.3 MPa·m$^{1/2}$ when crack bridging is present. In the present study, this effect may be even weaker due to the small grain sizes (< 1 μm); thus, the deflection path increasing around tiny grains is negligible. Therefore, the described mechanisms do not fully explain such high resistance to fracture.

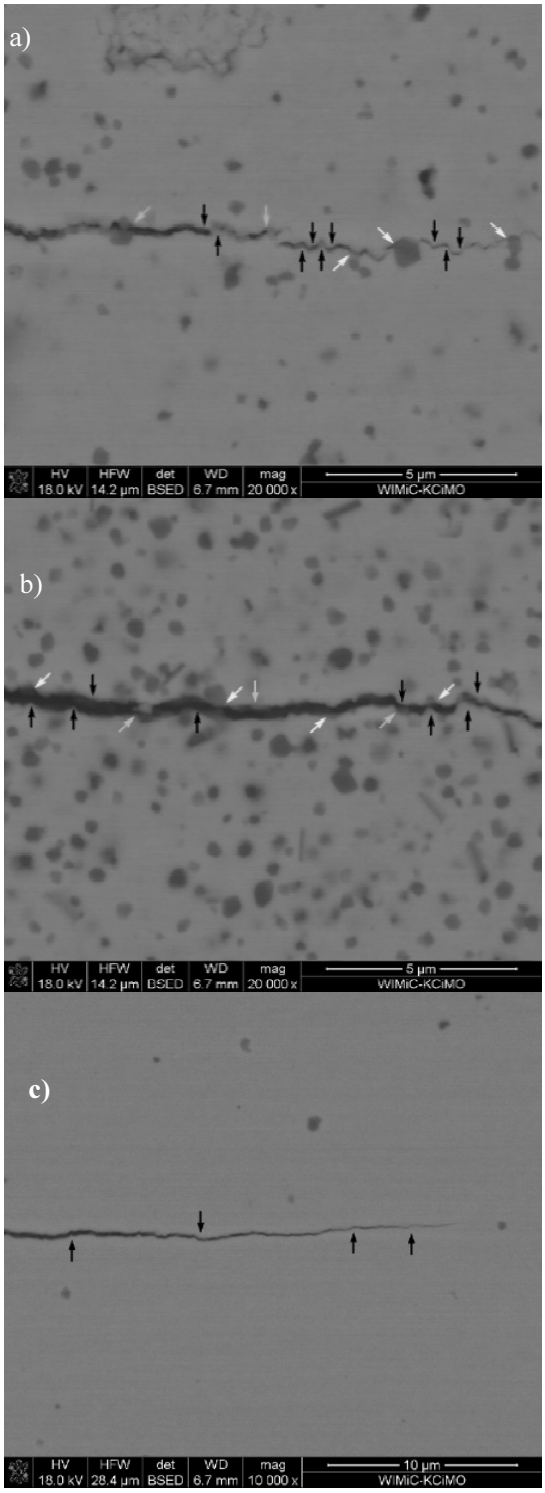

Fig. 3. Crack propagation path in: a) ATZ-B, b) ATZ-10 and c) T. Arrows indicate following mechanisms: black arrows – crack deflection; grey arrows – transgranular Al_2O_3 fracture; white arrows – boundary Al_2O_3 fracture propagation

 All rights reserved

Additionally, frequent changes in the fracture propagation directions of ahigh angle (close to even 90°) also contribute to toughness improvement [43]. The crack propagation rate in each deflected segment is related to distance d and angle θ of deflection from the straight span and those to the stress vector and stress intensity factor k1 and k2 components (Fig. 4) [44]. This effect is illustrated in Figure 4 and it can be seen that the crack path in 3Y-TZP comparing to ATZ-10 is a way more rectilinear.

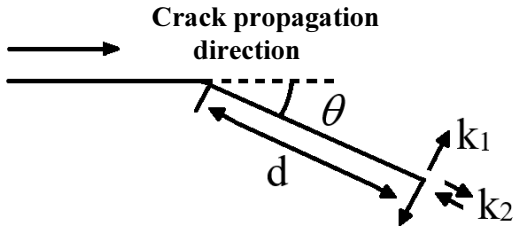

Fig. 4. Crack deflection angle θ from straight span, spanning distance d, and stress intensity factor components k1 and k2 (according to [44])

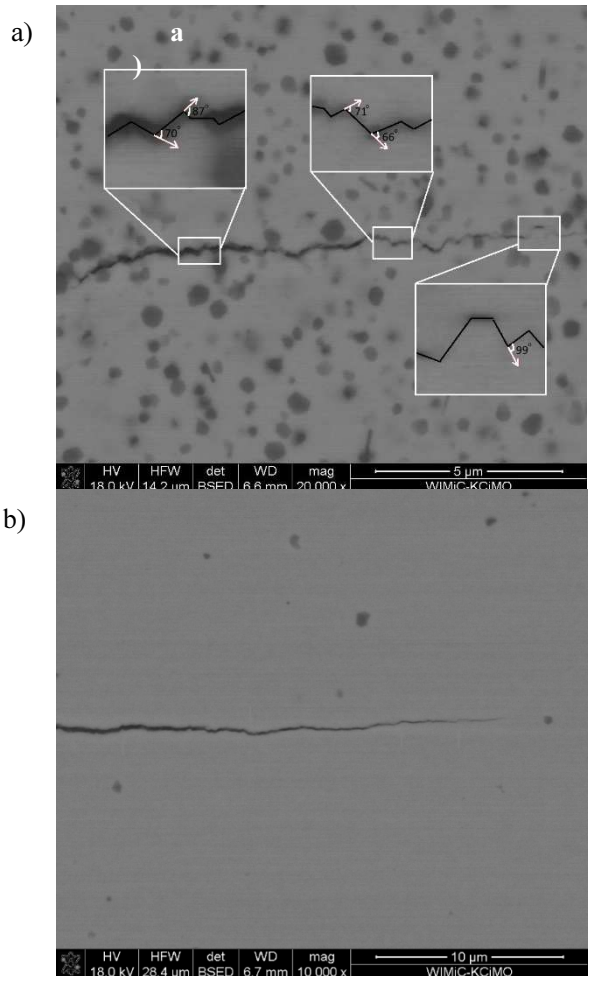

Fig. 5. Crack propagation path deviation for: a) ATZ-10 and b) T

As was mentioned above, the Young's modulus for pure Al_2O_3 and ZrO_2 monoliths are approximately 400 and 210 GPa, respectively. Consequently, it can be concluded, that the stiffness of the alumina grains should be twice as high as that of the zirconia grains. Thus, theoretically, for a crack that propagates in the ATZ material by the least energy-consuming route, it is impossible to run through the highly durable corundum grains. However, when the crack propagates in the investigated ATZ composite, its front passes through the Al_2O_3 particles or spreads along their boundaries (Fig. 3). The stress fields in the composite matrix attract the crack towards the Al_2O_3 particles. Levin et al. [45] stated that the occurrence of local compressive microstresses adjacent to the Al_2O_3 grain boundaries are required to direct the crack towards the Al_2O_3 inclusions. As was mentioned in introduction, those stress fields in ATZ composites come from the differences in the thermal expansions of ZrO_2 (10.5×10^{-6} K^{-1}) [46] and Al_2O_3 (8.8×10^{-6} K^{-1}) grain [46] phases, which during the cooling process create residual stress zones and also contribute to the creation of the fracture deflection path [47, 48]. Nevarez-Rascon [14] and Magnani et al. [27] confirmed the above reasoning and concluded that the stress field created through differences in thermal expansion does play a major role in creating the mechanism leading to the improvement in fracture toughening.

In the investigated ATZ composites, it can be assumed in line with the literature (Danilenko et al. [15] and many other authors such as Casellas et al. [49], Celli et al. [26] and Huang et al. [50]) that the main toughening mechanism is the tetragonal-monoclinic transition of the ZrO_2 phase, especially for the fine microstructure where this mechanism appears more to be intense and has a more dominant participation [27, 51]. Due to the specific method of preparation, an intensification of diffusion during sintering and strong ZrO_2 grain-to-grain interactions occurred. This phenomenon is additionally enhanced in ATZ-B by the small addition of Al_2O_3 inclusions [52-54]. Therefore, the ZrO_2 grains in the ATZ composites are characterized by particularly high transformability, which is a decisive factor for such high improvement in the fracture toughness. An increase in the Al_2O_3 phase content in ATZ-10 firstly reduces the contribution of this mechanism (a decrease in the high-transformable ZrO_2 phase content) and secondly, it makes the microstructure coarser as Al_2O_3 is characterized by larger grains (Table 3). The K_{1C} of the traditional, less transformable tetragonal ZrO_2 phase in reference material 3Y-TZP with a coarser microstructure was almost two times lower.

CONCLUSIONS

The investigated ATZ composites were prepared from two zirconia powders differing in Y_2O_3 content. The specific method of obtaining and optimizing the sintering conditions resulted in a fine, dense microstructure and uniquely improved the mechanical properties, especially oriented towards increasing the fracture

toughness. The K_{1C} parameter for the ATZ-B composite reached an outstanding value of 12.7 MPa·m$^{1/2}$, while for ATZ-10 a slight decrease in the fracture toughness was noticed (K_{1C} = 9.8 MPa·m$^{1/2}$). Nevertheless, this was a nearly twofold improvement in resistance to crack propagation compared to the 3Y-TZP reference material (K_{1C} = 5.1 MPa·m$^{1/2}$). The crack propagation path analysis revealed the presence of a crack deflection mechanism and mixed transgranular-intragranular crack propagation (crackbridging process) in both the investigated ATZ composites. The passage of the crack through the alumina inclusions was associated with the specific stress distribution present in the structure. Not withstanding, the presence of a highly transformable t-ZrO_2 phase in the fine-grained microstructure was the main toughening factor in the investigated ATZ composites. The high transformability and strong interactions between the ZrO_2 grains enables the attainment of a new level of crack inhibition mechanisms and an increase in the fracture toughness of the investigated ATZ ceramics.

REFERENCES

[1] Garvie R.C., Hannink R.H., Pascoe R.T., Ceramic steel? Nature 1975, 258, 703-704.

[2] Kelly J.R., Denry I., Stabilized zirconia as a structural ceramic: an overview, Dent. Mater. 2008, 24, 289-298.

[3] Bhattacharyya S., Agrawal D.C., Microstructure and mechanical properties of ZrO_2-Gd_2O_3 tetragonal polycrystals, Mater. Sci. 2002, 37, 7, 1387-1394.

[4] Lee D.Y., Kim D., Cho D., Low-temperature phase stability and mechanical properties of Y_2O_3- and Nb_2O_5-co-doped tetragonal zirconia polycrystal ceramics, Mater. Sci. 1998, 17, 3, 185-187.

[5] Khor K.A., Yang J., Lattice parameters, tetragonality (c/a) and transformability of tetragonal zirconia phase in plasma sprayed ZrO_2-Er_2O_3 coatings, Mater. Lett. 1997, 31, 23-27.

[6] Denry I., Kelly J.R., State of the art of zirconia for dental applications, Dental Materials 2008, 24, 3, 299-307, DOI: 10.1016/j.dental.2007.05.007.

[7] Piconi C., Maccauro G., Zirconia as a ceramic biomaterial, Biomaterials 1999, 20, 1, 1-25, DOI: 10.1016/s0142-9612(98)00010-6.

[8] Nevarez-Rascon A., Aguilar-Elguezabal A., Orrantia E., Bocanegra-Bernal M.H., Compressive strength, hardness and fracture toughness of Al_2O_3 whiskers reinforced ZTA and ATZ nanocomposites: Weibull analysis, Int. J. Refract. Met. Hard. Mater. 2011, 29, 3, 333-340, DOI: 10.1016/j.ijrmhm.2010.12.008.

[9] Correa de Sá e Benevides de Moraes M.C., Benavides de Moraes S., Elias C.N., Filho J., Guimarães de Oliveira L., Mechanical properties of alumina-zirconia composites for ceramic abutments, Mater. Research 2004, 7, 4, 643-649.

[10] De Aza A.H., Chevalier J., Fantozzi G., Crack growth resistance of alumina, zirconia and zirconia toughened alumina ceramics for joint prostheses, Biomaterials 2002, 23, 937-945.

[11] Hamadouche M., Sedel L., Ceramics in orthopaedics, J. Bone Jt. Surg. Br. 2000, 82, 1095-1099, DOI: 10.1302/0301-620X.82B8.11744.

[12] Shekhawat D., Singh A., Banerjee M.K., Singh T., Patnaik A., Bioceramic composites for orthopaedic applications: A comprehensive review of mechanical, biological, and microstructural properties, Ceramics Int. 2021, 47, 3, 3013-3030, DOI: 10.1016/j.ceramint.2020.09.214.

[13] Uhlířová T., Pabst W., Phase mixture modeling of the grain size dependence of Young's modulus and thermal conductivity of alumina and zirconia ceramics, J. Eu. Ceram. Soc. 2020, 40, 8, 3181-3190, DOI: 10.1016/j.jeurceramsoc.2020.01.069.

[14] Nevarez-Rascon A., Aguilar-Elguezabal A., Orrantia E, Bocanegra-Bernal M.H., On the wide range of mechanical properties of ZTA and ATZ based dental ceramic composites by varying the Al_2O_3 and ZrO_2 content, Int. J. Refract. Met. Hard. Mater. 2009, 27, 6, 962-970, DOI: 10.1016/j.ijrmhm.2009.06.001.

[15] Danilenko I., Konstantinova T., Volkova G., Burkhovetski V., Glazunova V., The role of powder preparation method in enhancing fracture toughness of zirconia ceramics with low alumina amount, J. Ceram. Sci. and Tech. 2015, 06, 3, 191--200.

[16] Abbas M.K.G., Ramesh S., Sara Lee K.Y., Wong Y.H., Ganesan P., Ramesh S., Alengaram U.J., Treng W.D., Purbolaksono J., Effects of sintering additives on the densification and properties of alumina-toughened zirconia ceramic composites, Ceram.- Int. 2020, 46, 27539-27549.

[17] Gregorová E., Semrádová L., Sedlářová I., Nečina V., Hříbalová S., Pabst W., Microstructure and Young's modulus evolution during re-sintering of partially sintered alumina-zirconia composites (ATZ ceramics), J. Eu. Ceram. Soc. 2021, 41, 6, 3559-3569, DOI: /10.1016/j.jeurceramsoc.2021.01.045.

[18] Kern F., Gadolinia neodymia co-stabilized zirconia materials with high toughness and strength, J. Ceram. Sci. Tech. 2012, 3, 3, 119-130, 10.4416/JCST2012-00004.

[19] Anstis G.R., Chantikul P., Lawn B.R., Marshall D.B., A critical evaluation of indentation techniques for measuring fracture toughness: I, direct crack measurements, J. Am. Ceram. Soc. 1981, 64, 533-543, DOI: 10.1111/j.1151-2916.1981.tb10320.x.

[20] Ying S., Rhee Y., Kang S., Experimental evaluation of toughening mechanism in alumina-zirconia composites, J. Am. Ceram. Soc. 1999, 82, 5, 1229-1232.

[21] Tuan W.H., Chen R.Z., Wang T.C., Cheng C.H., Kuo P.S., Mechanical properties of Al_2O_3/ZrO_2 composites, J. Eur. Ceram. Soc. 2002, 22, 16, 2827-2833.

[22] Hannink R.H.J., Kelly P.M., Muddle B.C., Transformation toughening in zirconia-containing ceramics, J. Am. Ceram. Soc. 2000, 83, 3, 461-487.

[23] Karihaloo B.L. Contributions of t–m phase transformation to the toughening of ZTA. J. Am. Ceram. Soc. 1991, 74, 1703-1706, DOI: 10.1111/j.1151-2916.1991.tb07166.x.

[24] Rühle M., Stecker A., Waidelich D., Kraus B., In situ observations of stress-induced phase transformation in ZrO_2 containing ceramics. In: Claussen N., Rühle M., Heuer A., Advances in ceram., Sci. and Tech. of Zirconia II. Columbus: Am. Ceram. Soc. 1984, 256, 74.

[25] Green D.J., Critical microstructures for microcracking in Al_2O_3-ZrO_2 composites, J. Am. Ceram. Soc. 1982, 65, 610-614.

[26] Celli A., Tucci A., Esposito L., Palmonari C., Fractal analysis in alumina-zirconia composites, J. Eur. Ceram. Soc. 2003, 23,469-479.

[27] Magnani G., Brillante A., Effect of the composition and sintering process on mechanical properties and residual stresses in zirconia-alumina composites, J. Eu. Ceram. Soc. 2005, 25, 15, 3383-3392, DOI: 10.1016/j.jeurceramsoc.2004.09.025.

[28] Tekeli S., Fracture toughness (K_{1C}), hardness, sintering and grain growth behaviour of 8YSCZ/Al_2O_3 composites pro-

duced by colloidal processing, J. Alloys and Compounds 2005, 391, 1-2, 217-224, DOI: 10.1016/j.jallcom.2004.08.084.

[29] Chai J., Zhu Y., Shen T., Liu Y., Niu L., Li S., Jin P., Cui M., Wang Z., Assessing fracture toughness in sintered Al_2O_3-ZrO_2(3Y)-SiC ceramic composites through indentation technique, Ceramics Int. 2020, 46, 17, 27143-27149, DOI: 10.1016/j.ceramint.2020.07.194.

[30] Liu H.L., Huang C.Z., Teng X.Y., Wang H., Effect of special microstructure on the mechanical properties of nanocomposite, Mater. Sci. Eng. 2008, 487, 258-263.

[31] Sun X.D., Li J.G., Zhang M., Li X.D., Xiao Y.L., Liang Y., Mechanism of strengthening of Al_2O_3/SiC nanocomposites, Acta Metall. Sin. 1999, 35, 879-882.

[32] Grabowy M., Wilk A., Lach R., Pędzich Z., Hydrothermal aging of ATZ composites based on zirconia made of powders with different yttria content, Materials 2021, 14, 6418, DOI: 10.3390/ma14216418.

[33] Cheng M., Chen W., Measurement and determination of dynamic biaxial flexural strength of thin ceramic substrates under high stress-loading, Int. J. Mech. Sci. 2005, 47, 1212--1223, DOI: 10.1016/j.ijmecsci.2005.04.004.

[34] Test Method for Biaxial Flexure Strength (Modulus of Rupture) of Ceramic Substrates, ASTM F394-78, 1996.

[35] Dudek A., Lach R., Wojteczko K., Rutkowski P., Zientara D., Pędzich Z., Subcritical crack growth in oxide and non-oxide ceramics using the Constant Stress Rate Test, Process. App. Ceram. 2015, 9, 4, 187-191, DOI: 10.2298/PAC1504187W.

[36] Niihara K., A fracture mechanics analysis of indentation-induced Palmqvist crack inceramics, J. Mater. Sci. Lett. 1983, 2, 221-223.

[37] Maji A., Choubey G., Microstructure and mechanical properties of alumina toughened zirconia (ATZ), Mater. Today 2018, 5, 2, 7457-7465, DOI: 10.1016/j.matpr.2017.11.417.

[38] Sequeira S., Fernandes M.H., Neves N., Almeida M.M., Development and characterization of zirconia-alumina composites for orthopedic implants, Ceram. Int. 2017, 43, 1, 693-703.

[39] Quinn G.D., Fracture toughness of ceramics by Vickers indentation crack length method: A critical review, Ceram. Eng. Sci. Proceed. 2006, 27, 3, 45-62.

[40] Li J., Watanabe R., Fracture toughness of Al_2O_3-particle-dispersed Y_2O_3 partially stabilized zirconia, J. Am. Ceram. Soc. 1995, 78, 4, 1079-1082.

[41] Faber K.T., Evans A.G., Crack deflection processes-I. Theory, Acta Metall. Mater. 1983, 31, 4, 165-176.

[42] Evans A.G., Perspective on the development of high-toughness ceramics, J. Am. Ceram. Soc. 1990, 73, 2, 187-205.

[43] Suresh S., Crack deflection: implications for the growth of long and short fatigue cracks, Metall Trans. A. 1983, 14, 2375-2385.

[44] Bilby B.A., Cardew G.E., Howard I.C., Stress intensity factors at the tips of kinked and forked cracks. In: Taplin D.M.R. (ed.), Analysis and Mechanics, Pergamon, 1978, 197-200, DOI: 10.1016/B978-0-08-022142-7.50039-9.

[45] Levin I., Kaplan W., Brandon D., Layyous A., Effect of SiC submicrometer particle size and content on fracture toughness of alumina-SiC "nanocomposites", J. Am. Ceram. Soc.1995, 78, 1, 254-256

[46] Kwon N.-H., Kim G.-H., Song H.S., Lee H.-L., Synthesis and properties of cubic zirconia-alumina composite by mechanical alloying, Mater. Sci. Eng. A 2000, 299, 185-194, DOI: 10.1016/S0921-5093(00)01376-9.

[47] Gil-Flores L., Salvador M.D., Penaranda-Foix F.I., D`almau A., Fernandez A., Borrell A., Tribological and wear behavior of alumina toughened zirconia nano-composites obtained by pressureless rapid microwave sintering, J. Mech. Behav. Biomed. Mater. 2019, 101, 103415, DOI: 10.1016/j.jmbbm.2019.103415.

[48] Zhang F., Li L.F., Wang E., Effect of micro-alumina content on mechanical properties of Al_2O_3/3Y-TZP composites, Ceram. Int. 2015, 41, 12417-1242.

[49] Casellas D., Rafols I., Llanes L., Anglada M., Fracture toughness of zirconia-alumina composites, Int. J. Refract. Met. Hard. Mater. 1999, 19, 11-20.

[50] Huang X.W., Wang S.W., Huang X.X., Microstructure and mechanical properties of ZTA fabricated by liquid phase sintering, Ceram. Int. 2003, 29, 765-769.

[51] Yoshimura M., Yashima M., Noma T., Somiya S., Formation of diffusionlessly transformed tetragonal phases by rapid quenching of melts in ZrO_2-RO1.5 systems (R = rare earths), J. Mater. Sci. 1990, 25, 4, 2011-2016.

[52] Matsui K., Ohmichi N., Ohgai M., Enomoto N., Hojo J., Sintering kinetics at constant rates of heating: Effect of Al_2O_3 on the initial sintering stage of fine zirconia powder, J. Am. Ceram. Soc. 2008, 88, 12, 3346-3352.

[53] Matsui K., Yoshida H., Ikuhara Y., Phase-transformation and grain-growth kinetics in yttria-stabilized tetragonal zirconia polycrystal doped with a small amount of alumina, J. Eur. Ceram. Soc. 2010, 30, 7, 1679-1690.

[54] Guo X., Yuan R., Roles of alumina in zirconia-based solid electrolyte, Journal of Materials Science 1995, 30, 4, 923--931.

 All rights reserved